Characterization and *n*-heptane cracking/isomerization catalysis of tungsten oxynitrides on EMT zeolite

S. Sellem [a], C. Potvin [a], J.-M. Manoli [a], J. Maquet [b] and G. Djéga-Mariadassou [a,1]

[a] *Laboratoire Réactivité de Surface, CNRS URA 1106, Casier 178, and*
[b] *Laboratoire Chimie de la Matière Condensée, CNRS URA 1466,*
Université P. & M. Curie, 4 Place Jussieu, 75252 Paris Cedex 05, France

Received 19 February 1996; accepted 23 April 1996

Catalysts made of two tungsten precursors (one of them containing phosphorus) impregnated on EMT zeolite were nitridated in flowing pure ammonia and passivated by O_2 (1 vol%) in an Ar stream leading to tungsten oxynitrides/EMT (W_2N/EMT) and phosphotungsten oxynitrides/EMT (PW_2N/EMT). The catalysts were examined by X-ray diffraction, NMR spectroscopy, transmission electron microscopy and energy dispersive X-ray spectroscopy. The materials were tested for the cracking/isomerization of *n*-heptane at atmospheric pressure and 623 K. Cracking ($C_3 + C_4$) was the major (about 90%) *n*-heptane reaction for all the catalysts. The influence of EMT supercages upon selectivity was observed. The yield of *n*-heptane isomers was significantly enhanced for W_2N/EMT and principally for PW_2N/EMT showing a higher hydrogenation function.

Keywords: hexagonal faujasite (EMT); tungsten oxynitrides/EMT catalysts; characterization (XRD, NMR, TEM, STEM/EDX); heptane cracking/isomerization

1. Introduction

In recent years an increasing interest has been developed in exploring the catalytic properties of early transition metal nitrides or carbides for reactions traditionally catalyzed by noble metals. Volpe and Boudart [1] have prepared Mo_2N and W_2N with high surface area by temperature programmed method in which a precursor oxide was treated in flowing ammonia as the temperature was progressively raised. Several oxynitrides of molybdenum and tungsten have also been reported and characterized following the traditional oxide routes or using polyanion precursors (ammonium paratungstate) [2]. Considering a similar approach, we have prepared tungsten oxynitrides using water soluble polyanionic precursors [3].

Little attention has been paid to the catalytic properties of early transition metal nitrides on various supports. Nagai et al. [4] have underlined that molybdenum nitrides supported on alumina were extremely active in the HDS of dibenzothiophene and in the HDN of carbazole [5]. These results have encouraged an investigation of supported tungsten oxynitrides. An hexagonal polytype of the Y cubic faujasite, named EMT, was chosen. Recently synthesized in a pure form [6], this zeolite exhibits a more open structure [7] and a highest Si/Al ratio leading to a stronger acidity [8] than the Y cubic zeolite.

This paper reports on the characterization of supported tungsten oxynitrides, including the influence of phosphorus, and their catalytic performance for the molecular probe reaction of *n*-heptane cracking–isomerization.

2. Experimental

2.1. Materials

The polyanionic precursor, $(NH_4)_6H_2W_{12}O_{40}$ (denoted as AMW), was purchased from Fluka. The phosphorus polyanion $(NH_4)_6P_2W_{18}O_{62}$ (denoted as APW) was synthesized [3].

Hexagonal faujasite zeolite (EMT) was prepared using 18-crown-6 as template material [6]. The synthesized material was calcined in air to remove the organic template [8]. The zeolite was converted to ammonium form by ion exchange with a 1 mol ℓ^{-1} (10 cm^3/g of zeolite) ammonium acetate solution for 24 h. The exchange is repeated three times. At this point almost 75% of the Na^+ ions are exchanged (Na/Al = 0.26), the exchanged zeolite is designated as $(Na)_{0.25}(NH_4)_{0.75}$EMT.

The hydrocarbon *n*-heptane used as reactant was Fluka purity. Gases: H_2 (purity: 99.5%), Ar (purity: 99.998%), He (purity: 99.5%), O_2 (purity: 99.5%) and NH_3 (purity: 99.96%) were purchased from the Air liquide Company. Catalysts were prepared by incipient wetness impregnation of the EMT zeolite.

The supported oxynitrides were prepared by nitriding the impregnated samples with flowing ammonia using a modification of the protocol described by Volpe and Boudart [1]. Some treatment parameters were changed

[1] To whom correspondence should be addressed.

to preserve the structural crystallinity of the zeolite support. Initially the sample (1 g) was linearly heated under flowing Ar (10 ℓ/h) from room temperature (RT) to 423 K at 60 K/h and held 1 h at 423 K. The temperature was then linearly increased from 423 to 773 K at 150 K/h and held for 0.5 h at 673 K. For the last step the temperature was finally increased from 673 to 973 K at 30 K/h, maintained for 4 h at 973 K, then cooled down to RT, always under flowing ammonia. The sample was then flushed with argon and passivated by O_2 (1 vol%) in the Ar stream (9 ℓ/h) for 1 h. The resulting materials were stored in vacuum. Before XRD and NMR measurements, the zeolite samples were allowed to rehydrate at ambient temperature in constant humidity.

The data reported table 1 indicate the main characteristics of the initial and nitridated EMT zeolites (denoted as EMT/NH_3) with the loaded samples obtained from AMW (denoted as W_2N/EMT) and PMW (denoted as PW_2N/EMT). As can be seen from table 1, chemical analysis revealed that the tungsten contents of the two catalysts are slightly different.

2.2. Techniques

2.2.1. X-ray diffraction

A Siemens D-500 automatic diffractometer was used (Cu K_α radiation) for the X-ray diffraction (XRD) powder patterns of the various solid phases. The degree of X-ray crystallinity of the loaded zeolites was estimated from the intensity of all reflections in the range $2\theta = 14.5$–$29.3°$ [9] and compared with those of the calcined NaEMT zeolite. For catalyst containing tungsten phases the measured crystallinity must be corrected [10] to assess the crystallinity of the EMT fraction (table 1).

2.2.2. NMR spectroscopy

The ^{29}Si and ^{27}Al MAS NMR spectra were recorded on Bruker MSL 400 (at 79.5 MHz) and MSL 300 (at 78.2 MHz) spectrometers respectively. ^{29}Si MAS spectra were measured with 2 μs (equivalent to $\pi/4$) radiofrequency pulses, 10 s recycle delays using rotor spinning rate of 5 kHz and 2000 to 20000 scans cumulated. ^{29}Si chemical shifts are quoted in ppm from external tetramethylsilane as a reference. The ^{27}Al spectra were recorded with 1 μs radiofrequency pulses and 0.3 s recycle delays, spectral window 1 MHz. MAS rotors were spun at 15 kHz, the number of accumulated decays ranged from 300 to 3000. ^{27}Al chemical shifts are given in ppm from external $Al(H_2O)_6^{3+}$. Values of Si/Al obtained are reported in table 1.

2.2.3. Transmission electron microscopy

Samples for characterization by STEM-EDX or by TEM were prepared by two methods: direct dispersion and ultramicrotomy. The specimens were loaded into a Jeol (JEM 100CXII) transmission scanning electron microscope equipped with an ASID 4D (STEM mode). The operating voltage was 100 kV. Energy-dispersive X-ray analyses (EDX) were carried out using a LINK AN10000 system. The HRTEM observations and selected area electron diffractions were performed with a Jeol apparatus (JEM 100CXII) equipped with a top-entry device and operating at 100 kV accelerating voltage.

2.3. Molecular probe reactions

The *n*-heptane isomerization/cracking reaction was carried out over 70 mg of catalyst in a flow reactor at 623 K at a total pressure of 1 bar. The reaction feed was a mixture of hydrogen and nC_7 in a ratio of 18 to 1, the total gas flow being 0.72 ℓ/h. The sample was first pretreated at 773 K under flowing hydrogen for 5 h and then cooled down to 623 K. The protonic form was generated from the ammonium one by the previous in situ pretreatment leading principally to Brønsted acidity. The reaction products were separated and identified by an on-line HP chromatograph, equipped with a 50 m PLOT capillary column coated with alumina deactivated by KCl (temperature programmed from 353 to 473 K) and a FID detector.

3. Results and discussion

3.1. Characterization of supported catalysts

3.1.1. X-ray crystallinity

All X-ray diffraction peaks appearing in the diffractograms of the starting EMT zeolite were also present in

Table 1
Characteristics of catalyst compounds

Materials	W loading (%)	Crystallinity		Si/Al	
		obs.	cor.	anal.	NMR
$(Na)_{0.25}(NH_4)_{0.75}$EMT		105		3.6	3.7–3.8 [b]
EMT/NH_3		96		–	4.6 [a]–4.9 [b]
W_2N/EMT	12.4	60	98	3.8	4.3 [a]–4.7 [b]
PW_2N/EMT	13.1	56	94	3.7	4.4 [a]–4.6 [b]

[a] After NH_3 treatment.
[b] After subsequent activation (773 K) under H_2.

the patterns of the loaded EMT catalysts. As can be seen no noticeable decrease of crystallinity is induced after impregnation and nitridation treatment. Nevertheless, broad peaks were detected at $2\theta = 38°$ and 44°. Such diffraction lines are in agreement with the major ones of βW_2N phase type structure (JCPDS 25-1257).

3.1.2. NMR spectroscopy

Fig. 1 shows ^{29}Si MAS and ^{27}Al MAS selected NMR spectra for non-loaded zeolites and tungsten oxynitrides/EMT. The ^{29}Si spectra of $(Na)_{0.25}(NH_4)_{0.75}EMT$ (fig. 1a) consists of four lines centered at −90, −95, −101 and −106.5 ppm and corresponding respectively to Si(3Al), Si(2Al), Si(1Al) and Si(0Al) environments. The relative intensities of lines allow us to calculate a global Si/Al ratio of 3.6 (table 1). Activation in flowing H_2 at 773 K (catalytic pretreatment conditions) leads to a protonated form and to a slight enhancement of the Si/Al ratio (fig. 1b). Furthermore, nitridation and subsequent catalytic pretreatment on the unloaded zeolite give rise to a broadening of the spectra and to a disappearance of the signals at −90 and at −95 ppm indicating a partial destruction of the framework (table 1).

In contrast the spectra for the loaded EMT zeolite, after nitridation and activation, are well defined and show an increase of the Si/Al ratio from 3.6 to 4.7 (fig. 1c) for W_2N/EMT and 4.6 for PW_2N/EMT. Thus the impregnation and subsequent nitridation of the loaded zeolite seem to prevent advantageously the partial collapse of the zeolite framework.

Concerning the ^{27}Al MAS NMR spectra of the initial sample only the presence of tetrahedral Al ($\delta = 58$–60 ppm) is observed (fig. 1d). After nitridation the resonance from four-coordinated Al is markedly broadened indicating the presence of non-framework aluminum distorted and/or five-coordinated environment of aluminum. After activation, similar trends occur leading to a significant amount of octahedral extra-framework aluminum (fig. 1e, signal from 0 to 4 ppm). The tungsten oxynitrides supported samples behave similarly after identical treatments, with broad lines located at about 30–40 ppm coming from an intermediary chemical status of aluminum (fig. 1f). The difference between the Si/Al ratios before and after NH_3 treatment allows one to calculate approximately the extra-framework aluminum for the non-loaded zeolite: nitridation leads to the extraction of 3.5 framework Al per unit cell forming non-framework aluminum (Si/Al increasing from 3.6 to 4.6). Subsequent activation increases this value by 0.7 (Si/Al from 4.6 to 4.9). A similar conclusion can be deduced for the loaded samples (Si/Al increasing from 3.6 to 4.3 by nitridation and from 4.3 to 4.7 after activation for W_2N/EMT).

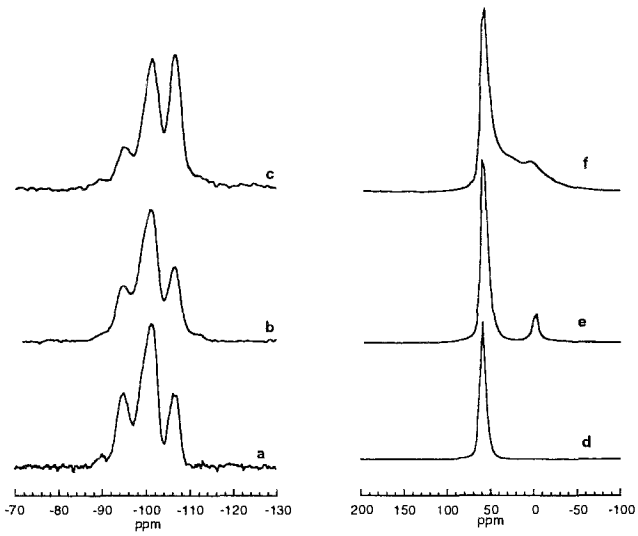

Fig. 1. ^{29}Si MAS NMR spectra: (a) $(Na)_{0.25}(NH_4)_{0.75}EMT$; (b) $(Na)_{0.25}(NH_4)_{0.75}EMT$ activated (H_2, 773 K); (c) W_2N/EMT activated. ^{27}Al MAS NMR spectra: (d) $(Na)_{0.25}(NH_4)_{0.75}EMT$; (e) $(Na)_{0.25}(NH_4)_{0.75}EMT$ activated; (f) W_2N/EMT activated.

So our NMR results indicate that Lewis acid sites (related to extra-framework aluminum) are to be considered with Brønsted acid sites (related to SiOHAl groups of the framework) in catalytic acid activities.

3.1.3. Proof of the presence of tungsten oxynitrides particles

As shown in fig. 2, black spots are observed corresponding to quite small particles, with sizes ranging between 12 and 20 Å. Other electron micrographs also showed few larger particles, presenting the same aspect, but deposited on the external surface of the zeolite grains attributed to tungsten oxynitrides according to their electron microscopic patterns. The HRTEM micrographs on thin cuts did not reveal any severe damage of the zeolite lattice, fringes of EMT lattice are quite visible on fig. 2

EDX performed on thin cut sections showed that in addition to aluminum and silicon, W_L lines appeared even in the case where spots are not visible. As the $W_{M\alpha}$ and $Si_{K\alpha}$ lines overlap, the determination of tungsten on the nitridated catalysts relied on the intensity of W_L. A similar observation using EDX has also been previously made for Y zeolite impregnated with ammonium metatungstate [11]. After tungsten–silicon overlap correction, W/Al atomic ratios going from 0.05 to 0.2 were found for all the examined cuts.

These observations clearly show that tungsten oxynitrides particles are well distributed throughout the zeolites. Thicker particles being also present on the surface and in the cracks of the zeolites grains.

3.2. Catalytic runs

The dependence of the *n*-heptane total conversion (defined as number of moles of nC_7 transformed for 100 moles of nC_7) on time-on-stream for all materials investigated (runs at 623 K) is shown in fig. 3. The conversion falls rapidly over the first 50 min, then decays slowly from 50 to 370 min on stream.

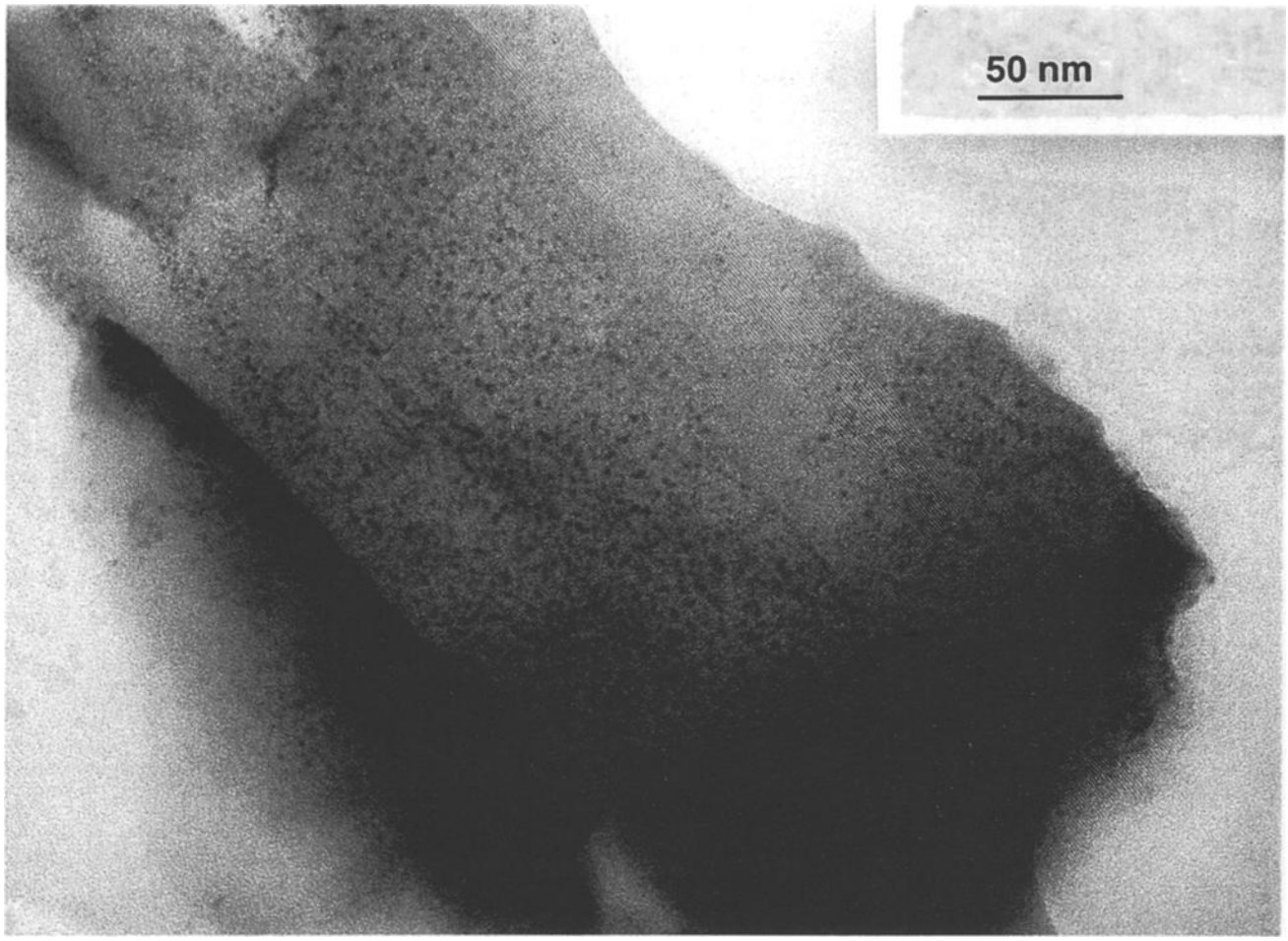

Fig. 2. HREM micrograph of thin cut of tungsten oxynitride/EMT.

Results on product distribution (moles for 100 moles of products obtained) quoted for a conversion of 6.7% (activity: 1.6 mmol h^{-1} g^{-1}) representing essentially steady-state conversion levels, are presented table 2. Cracking ($C_3 + C_4$) and isomerization selectivities are defined in fraction of 100 moles of nC_7 converted into $C_3 + C_4$ (cracking) or isoheptanes (isomerization).

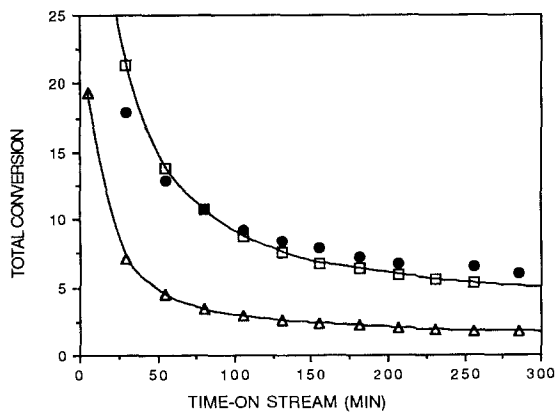

Fig. 3. Plot of total conversion versus time-on-stream for *n*-heptane at 623 K for: (□) EMT; (△) EMT/NH_3; (●) PW_2N/EMT.

With the non-loaded EMT, cracking is the most significant reaction; however, the formation of *n*-heptane isomers can be observed [12], global product distribution being similar for all catalysts. At the beginning of the reaction propane and isobutane constitute the main cracking products, while isomerization yields mainly methylhexanes. Traces of ethane and toluene are also observed.

The same type of result was observed on the fully exchanged EMT, obtained according to the procedure of Dougnier et al. [12]. A sample of LZY64 (IZA structure type FAU, Si/Al = 2.4) obtained from UOP was also examined in the cracking of *n*-heptane under the same catalytic conditions. Conversion after 5 min time-on-stream is still in favour of EMT.

Nitridation of unloaded $(Na)_{0.25}(NH_4)_{0.75}$EMT leading to EMT/NH_3 has a drastic effect on the activity of the zeolite (fig. 3). The results obtained here indicate that dealumination induced by ammonia (fig. 1) led to a decreasing of catalytic activity by blocking pores and acid sites.

Thus it is clear, as would be expected with acidic catalysts, that the classical acidic catalytic sequence in which the *n*-heptyl carbenium ions are isomerized

Table 2
Products distribution and selectivity (mol%) for *n*-heptane isomerization/cracking reaction at 623 K determined for a conversion of 6.7% (activity of 1.6 mmol h^{-1} g^{-1})

Products	EMT	EMT/NH_3	W_2N/EMT	PW_2N/EMT
propane	27.5	24.8	34.6	37.5
propene	19.3	23.0	13.4	10.9
isobutane	37.6	34.7	36.5	34.9
butane	3.7	3.7	4.4	5.2
butenes	5.3	7.3	4.7	4.9
isopentanes	2.7	3.2	2.1	2.0
pentane		0.7	0.3	0.4
m-pentane	0.8	0.9	0.6	0.5
isoheptanes	0.3	0.4	0.3	0.3
2-MH and 3-MH [a]	2.8	1.2	3.1	3.2
molar ratio				
propane/propene	1.4	1.1	2.6	3.4
$isoC_4/nC_4$	10.3	9.4	8.2	6.7
%crack. ($C_3 + C_4$) [b]	89.1	90.0	89.2	89.2
$\%isoC_7$ [b]	5.9	3.1	6.5	6.7

[a] 2-MH: 2-methylhexane; 3-MH: 3-methylhexane.
[b] Selectivity for 100 moles of nC_7 transformed.

through protonated cyclopropane intermediates and undergoing subsequent β-scission is dominating [13].

Branched-to-linear C_4 ratio presents always a high value from 7 to 11 after 340 min on stream, significantly exceeding the thermodynamic value (0.8 at 623 K). Higher yields of isoproducts have recently been reported in C_{16} hydrocracking [14] and C_6 cracking [15] over EMT-based catalysts. The high value of iC_4/nC_4 indicates that the supercages present in the EMT zeolite play an important role in the cracking behaviour of the material. Indeed it is accepted from a general cracking mechanism [16] that isobutane should be formed by the fast β-scission of 2,2'-dimethylpentane carbenium ion and by saturation of isobutene by hydrogen transfer. Thus the formation of the relatively large 2,2'-dimethylpentane isomer can occur better in the large cavities. Furthermore, the hydrogen transfer reaction involving isobutene is favoured by a better accessibility of the acid sites. Moreover, the propane/propene ratio decreases with catalyst deactivation. This ratio is also a measure of the hydrogen transfer ability of cracking catalysts, which on the other hand depends on pore dimensions and acid sites accessibility.

Bulk tungsten oxynitrides alone present a bifunctional behaviour as already reflected in the *n*-heptane molecular probe reaction [3]. For tungsten oxynitrides supported on EMT, the challenge can be to bring the hydrogenating function of the oxynitrides.

As reflected by the catalytic runs on supported oxynitrides, cracking products ($C_3 + C_4$) remain in majority, smaller amounts of olefinic C_3 and C_4 are now observed, while isomerization is enhanced (C_7 molecules). An increase in the isomerization selectivity appeared also now, reaching a value of 6.7% with PW_2N/EMT for 100 moles of nC_7 converted (table 2).

This result is in line with the lowest selectivity in methylhexanes of EMT/NH_3 now increased by the positive influence of the supported tungsten oxynitrides which favour the isomerization selectivity.

The $isoC_4/nC_4$ ratio in every cracked ratio decreases from 10.3 with the protonated form of $(Na)_{0.25}(NH_4)_{0.75}$EMT to 6.7 for PW_2N/EMT for an activity of 1.6 mmol h^{-1} g^{-1} (table 2). The paraffin/olefin C_3 ratio is now about two or three times greater than for the unloaded zeolites. These parallel results suggest a significant hydrogenation function of the dispersed tungsten oxynitrides.

A clear trend for the selectivity of C_7 isomers with decreasing heptane conversion is observed. The acidic sites are less active at low conversion level, the C_7 isomerization selectivity increases from EMT to PW_2N/EMT, the hydrogenating function being now enhanced.

All these observations indicate that these supported catalysts act as bifunctional catalyst with a small hydrogenating/acidic site ratio [17].

4. Conclusion

The claimed high acid strength of HEMT compared to HFAU, investigated by infrared techniques and benzene adsorption [8], is also reflected in the *n*-heptane reaction probe.

Starting from $(Na)_{0.25}(NH_4)_{0.75}$EMT zeolites, well-dispersed tungsten oxynitrides might be obtained with a good crystallinity. According to heptane tests, these materials behave as bifunctional catalysts as evidenced by isomerization selectivity. As in bulk tungsten oxynitrides the presence of phosphorus enhances the hydroge-

nating capacity. Nevertheless, these catalysts are not ideal bifunctional catalysts like Pt-containing zeolites, the hydrogenating function is here insufficient to allow a high selectivity of isomerization of heptane.

Further emphasis will be made to modify the acidity of the zeolite by dealumination inducing a better balance between acidic and hydrogenating functions.

Acknowledgement

The help of Mrs. P. Beaunier and Mr. M. Lavergne with the STEM-EDX measurements and the TEM is greatly appreciated.

References

[1] L. Volpe and M. Boudart, J. Solid State Chem. 59 (1985) 332.
[2] R. Kiessling and L. Peterson, Acta Metallurgica 2 (1954) 676.
[3] S. Sellem, C. Potvin, J.-M. Manoli, R. Contant and G. Djéga-Mariadassou, J. Chem. Soc. Chem. Commun. (1995) 359.
[4] M. Nagai and T. Miya, Catal. Lett. 15 (1992) 105.
[5] M. Nagai, T. Miya and T. Tubor, Catal. Lett. 18 (1993) 9.
[6] F. Delprato, L. Delmotte, J.L. Guth and L. Huve, Zeolites 10 (1990) 546.
[7] C. Baerlocher, L.B. McCusker and R. Chiappetta, Microporous Mater. 2 (1994) 269.
[8] B.L. Su, J.-M. Manoli, C. Potvin and D. Barthomeuf, J. Chem. Soc. Faraday Trans. 89 (1993) 857.
[9] T. Chatelain, J. Patarin, M. Soulard, J.L. Guth and P. Schulz, Zeolites 15 (1995) 90.
[10] J. Leglise, J.-M. Manoli, C. Potvin, G. Djéga-Mariadassou and J. Cornet, J. Catal. 152 (1995) 275.
[11] R. Cid, J. Neira, J. Godoy, J.M. Palacios, S. Mendioroz and A. Lopez-Agudo, J. Catal. 141 (1993) 206.
[12] F. Dougnier, J. Patarin, J.L. Guth and D. Anglerot, Zeolites 12 (1992) 160.
[13] F. Lemos, F.R. Ribero, M. Kern, G. Giannetto and M. Guisnet, Appl. Catal 29 (1987) 43.
[14] J.A. Martens and P.A. Jacobs, J. Mol. Catal. 78 (1993) L47.
[15] V. Zholobenko, A. Garforth, M. Mähkarova, J. Zhao and J. Dwyer, in: *Catalysis by Microporous Materials*, Stud. Surf. Sci. Catal., Vol. 94 (Elsevier, Amsterdam, 1995) p. 560.
[16] A. Corma, J. Planelles, J. Sanchez-Marin and F. Tomas, J. Catal. 93 (1985) 30.
[17] M. Guisnet, A. Alvarez, G. Giannetto and G. Pérot, Catal. Today 1 (1987) 415.